PHYSIOLOGIA PLANTARUM 113: 486–498. 2001
Printed in Ireland—all rights reserved

ISSN 0031-9317

Effects of aluminum in red spruce (*Picea rubens*) cell cultures: Cell growth and viability, mitochondrial activity, ultrastructure and potential sites of intracellular aluminum accumulation

Rakesh Minocha[a,*], Carolyn McQuattie[b], Wayne Fagerberg[c], Stephanie Long[a] and Eun Woon Noh[d]

[a]*USDA Forest Service, PO Box 640, 271 Mast Road, Durham, NH 03824-0640, USA*
[b]*USDA Forest Service, 359 Main Road, Delaware, OH 43015-8640, USA*
[c]*Department of Plant Biology, University of New Hampshire, Durham, NH 03824, USA*
[d]*Forest Research Institute, Biotechnology Division, Suwon 441-350, Republic of Korea*
**Corresponding author, e-mail: rminocha@hopper.unh.edu*

Received 6 December 2000; revised 5 June 2001

The effects of Al on red spruce (*Picea rubens* Sarg.) cell suspension cultures were examined using biochemical, stereological and microscopic methods. Exposure to Al for 24–48 h resulted in a loss of cell viability, inhibition of growth and a significant decrease in mitochondrial activity. Soluble protein content increased in cells treated with Al. Using energy-dispersive X-ray microanalysis on sections of freeze-substituted cells that had no obvious disruption in cytoplasmic or cell wall structure, Al (always in the presence of P) was detected in dense regions in cell walls, cytoplasm, plastids and vacuoles after 48 h exposure to Al. Stereological quantification of spruce cell structure showed that, after 24 h of Al treatment, intact cells had increased vacuolar and total cell volume, but the nuclear volume did not change. In addition, Al treatment resulted in increased surface area of Golgi membranes and endoplasmic reticulum. The biochemical and ultrastructural alterations in red spruce cells, in combination with the presence of Al in cellular organelles of visually intact cells, suggest that Al movement occurred across the plasma membrane without major cellular disruption. Detailed short-term time course studies are needed to determine if intracellular Al in these cells results from its passage into cells through submicroscopic lesions in the plasma membrane or it is taken up into the symplast through the intact membrane by an active, but slow, process.

Introduction

The adverse effects of acidic deposition on soil productivity, due to increased solubilization of aluminum (Al) and leaching of base cations, are of major concern to forest land managers because such processes may impact growth over large forested areas. Al has been shown to be toxic to plants and is responsible for reduced plant growth and productivity (Kochian 1995, Rengel 1996 and references therein). Major symptoms of plants and/or cell cultures exposed to Al include inhibition of DNA synthesis and cell division, premature vacuolation and disruptions in root meristem cells, reduced root growth and loss of biomass (McQuattie and Schier 1990, Schier et al. 1990, Minocha et al. 1992, 1996, Kinraide 1998, Lazof and Holland 1999). Previous work on the effects of Al in red spruce (*Picea rubens* Sarg.) cell cultures and in leaves of mature trees showed an inverse relationship between levels of cellular putrescine (a diamine that is a proposed indicator of stress) and Ca^{2+} and Mg^{2+} (Minocha et al. 1996, 1997). The specific biochemical and ultrastructural effects of Al on red spruce embryogenic cells are not known. In addition, whether Al enters the symplast of these cells and accumulates within discrete subcellular compartments has not been studied thus far.

Al alters permeability of the plasma membrane by causing changes in the properties of ion channels through interaction with channel proteins (Rengel 1992). Al also has been shown to alter the types of membrane lipids present and their peroxidation level (Rengel 1996 and references therein, Yamamoto et al. 1997, Zhang et al. 1997). However, it is

Abbreviations – EDX, energy-dispersive X-ray microanalysis; FS, freeze-substitution; MTT, [3-(4,5-dimethylthiazol-2-yl)-2,5-diphenyl tetrazolium bromide]; TEM, transmission electron microscopy.

unclear to what extent these changes in membrane permeability might alter Al uptake across the membrane. According to Taylor et al. (2000) the understanding of Al transport across the plasma membrane has been hampered by various factors, including problems with complete desorption of cell wall-bound Al by various solutions, the lack of an affordable and appropriate isotope of Al, the lack of a sensitive technique for detection of low levels of Al and the complex aqueous coordination chemistry of Al. An effective method to desorb Al from cell walls is necessary to estimate Al uptake into the symplast. Treatment of Al-treated *Chara* cells with a wide variety of desorbents for up to 5 h under stringent conditions was not able to completely desorb Al (Rengel 1996) thus proving that the ineffective desorption techniques may be one major cause for disagreement in the estimation of symplastic Al among various studies. In addition, analytical techniques used to detect or quantitate symplastic Al content in plant cells vary in sensitivity and resolution. Techniques used thus far, including secondary ion mass spectroscopy (SIMS), energy-dispersive X-ray microanalysis (EDX) technology, laser microprobe mass analysis, ^{27}Al nuclear magnetic resonance, accelerator mass spectroscopy (AMS) and colorimetric techniques, have been discussed at length (Lazof et al. 1994, Rengel 1996, Marienfeld et al. 2000, Taylor et al. 2000). It is difficult to make generalizations about intracellular Al localization because of the use of different instruments, sample preparation methods, operating conditions and lengths of Al exposure in various studies (Rengel 1996). Previous studies have indicated that Al may not be detected by EDX in the symplast during the first few hours after Al exposure due to sensitivity limitations of this technique (Lazof et al. 1994). In the present study, EDX was used in combination with freeze-substitution (FS) sample preparation to identify (but not quantitate) potential sites of Al accumulation in the subcellular components of cells treated with Al for more than 24 h.

It has been postulated that Al entry into the symplast may not be required for the primary toxic effects to occur from short-term treatment with Al (Olivetti and Etherton 1991, Huang et al. 1992, Rengel 1992). The plasma membrane has been documented in some studies (Cuenca et al. 1991, Marienfeld and Stelzer 1993, Marienfeld et al. 1995) to be an effective barrier to Al entry into the cytoplasm. However, other researchers have found that Al apparently enters the symplast and accumulates in root cells (Matsumoto et al. 1976, Zhang and Taylor 1989, Lazof et al. 1994, 1997). A lag phase between Al accumulation in the apoplast and the symplast has been suggested previously (Rengel 1992). Using SIMS technology, Rengel and Reid (1997) reported uptake of Al across the plasma membrane of *Chara* cells without any delay, but at a low rate that was directly proportional to Al concentration in the medium. However, 99% of the Al still was accumulated within the cell wall. The slow rate of transport to the symplast may explain the lag phase reported earlier for Al detection and/or accumulation between the cell wall and the symplast. Thus, depending on the technique used, Al, though present in the symplast in low levels after short-term exposure, may not be detected there until it reaches a certain critical threshold level. Al may be transported across the membrane as neutral complexes (possibly associated with P), and these would not depolarize the plasma membrane (Rengel 1992). Using EDX, Vázquez et al. (1999) demonstrated the presence of Al with P after 4 h of Al exposure in the cell walls and vacuoles of roots of an Al-tolerant maize variety. By 24 h, Al could not be detected in the cell walls, but the concentration of Al increased in the vacuoles of these cells. This finding is unique and may have to do with the resistance mechanism(s) of this species to Al since, in most published literature, a large portion of Al has been found to be associated with cell walls even in the long-term Al exposure studies. More recently, Taylor et al. (2000) used ^{26}Al isotope and AMS on *Chara* cells to demonstrate localization of Al in the symplast (within the first 30 min) and in the vacuoles where saturation levels were reached 12–24 h after exposure. The authors suggested (though with caution because their conclusions are based on speciation analyses of bulk solution which may not have much similarity with the membrane surface) that Al may have entered the symplast as a citrate or sulfate complex. Ma and Hiradate (2000) also reported transport of Al across the plasma membrane of buckwheat within 4 h of Al exposure, suggesting that Al transport may be a passive process with Al translocated as Al-citrate complex.

In this study, cell structure was measured by utilizing quantitative techniques (stereology). Stereological techniques used in this study extrapolate structural information from a population of two-dimensional micrographs to create a quantitative description of an average (mean) cell from a population of sampled cells in 3-dimensional terms (Weibel 1979, Steer 1981, Fagerberg 1988). These techniques allow one to quantitate cell structure, i.e., establish a ratio between the size of an organelle (e.g., its volume or surface area) and the volume of the whole cell. These ratios are derived from measurements taken from a large number of electron micrographs that are taken from the population of cells comprising the sample tissue. Since these data are quantitative, differences between samples can be subjected to statistical analysis for 'assumptions of correctness', and very small cytological changes between populations of cells can be detected (Fagerberg 1988). These data also can be correlated with other quantitative types of data, thereby linking structure with physiology and biochemistry.

The purpose of this work was to conduct a thorough analysis of the effects of Al on physical and biochemical changes in red spruce embryogenic cells after 24 and 48 h of Al exposure. Specifically, a series of experiments were undertaken to (1) study the effect of Al on cell viability, growth, and mitochondrial activity, (2) determine by transmission electron microscopy (TEM) the effect of Al on cell ultrastructure, (3) detect by EDX possible sites of Al accumulation in apoplastic or symplastic regions of cells and (4) quantify changes in cell organelles due to Al treatment.

Materials and methods

Culture conditions

Embryogenic suspension cultures of red spruce (cell line RS61.1, 03-92) were maintained in modified half strength Litvay's medium (Litvay et al. 1981) as described by Minocha et al. (1996). Briefly, the modifications include addition of 3.42 m*M* glutamine, 9.05 μ*M* 2,4-D, 4.44 μ*M* benzyladenine, 1.0 g l^{-1} casein hydrolysate and 2% (w/v) sucrose instead of 3% (w/v). In addition, iron supplement was provided either by adding 40 mg l^{-1} of the commercial plant product Sequestrine (Plant Products Company Ltd., Brampton, Ontario, Canada) containing 7% (w/v) Fe chelate or by addition of 7.25 μ*M* Fe-EDTA. The medium was adjusted to pH 5.7 before autoclaving. Cells were subcultured routinely at 7-day intervals by transferring 15 ml of cell suspension into 45 ml of fresh medium in 250-ml Erlenmeyer flasks. The flasks were incubated in the dark on a gyratory shaker (120 rpm) at 25 ± 2°C.

Experimental treatments

Seven-day-old cell suspensions were mixed with an equal volume of fresh medium in a Florence flask. Ten milliliters of this diluted cell suspension were transferred to individual 50-ml experimental flasks containing 10 ml of fresh medium (pH 5.7), thus providing a final cell density comparable to routine subcultures. Uniform distribution of cells was obtained by continuous stirring at low speed during the period of transfer to experimental flasks. Aluminum chloride ($AlCl_3$) (0, 0.2, 0.5 or 1.0 m*M*; 1.0 m*M* for biochemical analyses only) was added to 3-day-old cells maintained in 50-ml flasks, and the flasks were maintained under conditions described above for 24 or 48 h. The pH of the medium containing 3-day-old cells at the time of Al addition, was 4.2 ± 0.3. All treatments were run in triplicate or quadruplicate, and most experiments were repeated at least 3 times.

All of the ultrastructure studies were done on cells grown in growth media containing Sequestrine (described above) that precipitated a portion of free Al. In order to determine effective monomeric Al concentration in this situation, Al was either added to the cell-free medium or to 3-day-old cultures at a pH of 4.2 ± 0.3. In either case, about 55% (w/w) Al became insoluble. The precipitate was removed by centrifugation at 31400 *g* for 20 min and the supernatant analyzed for monomeric Al by the procedure of Driscoll (1984). The effective concentrations of monomeric Al in this medium were 0.09 and 0.23 m*M*, respectively, for 0.2 and 0.5 m*M* Al additions (Minocha et al. 1996). However, for the subsequent biochemical studies, Sequestrine was replaced with an equal quantity of iron in the form of Fe-EDTA (7.25 μ*M*), and thus the effective monomeric Al concentration was the same as the added concentration. No further analyses were performed to determine various active forms of monomeric Al. However, since the pH of the media was always below 4.5, we assumed that the monomeric Al existed primarily in the form of Al^{3+}.

Biochemical assays

Collection of cells

At 24 and 48 h after Al addition, cells were collected on Miracloth (Calbiochem-Behring Corp., La Jolla, CA, USA) and washed twice with an equal volume of growth media. After recording the total pellet fresh weight, cells were subdivided into fractions for Evans blue, [3-(4,5-dimethylthiazol-2-yl)-2,5-diphenyl tetrazolium bromide] (MTT) and protein assays as described below.

Quantitation of plasma membrane integrity by Evans blue uptake

Evans blue is a nonpermeating dye that can enter the cells only through damaged/ruptured plasma membranes and stain the contents of dead cells. It has been used in plant tissues as indicator of loss of plasma membrane integrity as well as cell death (Ikegawa et al. 1998). For Evans blue assay, cells (100 mg fresh weight) were transferred to 2-ml microfuge tubes and suspended in 0.05% (w/v in water) Evans blue solution and incubated for 15 min at room temperature. Cells were pelleted by centrifugation at 16000 *g* for 5 min and washed 5–6 times with distilled water until no more dye was eluted from the cells. The trapped dye was released by the addition of 1 ml of 1% sodium dodecyl sulfate (w/v in water) and ultrasonication (FS-14, Fisher Scientific, Pittsburgh, PA, USA) for 1 h at room temperature. For comparison, this step was also performed by sonicating the cells with a microprobe (as suggested by Ikegawa et al. 1998) or freeze-thawing the cells twice. All 3 methods yielded comparable results. The supernatant was obtained by centrifugation at 16000 *g* for 10 min. The supernatant was spectrophotometrically (Hitachi Instruments Inc., San Jose, CA, USA) analyzed at 600 nm for changes in optical density, which in turn reflected changes in plasma membrane integrity.

Quantitation of mitochondrial activity by MTT cleavage

The original procedure of Mosmann (1983) for mammalian cells as modified by Ikegawa et al. (1998) for plant cells was used for quantitation of mitochondrial activity after minor modifications as described below. Briefly, 1 ml of medium containing 250 μg MTT ml^{-1} was added to 100 mg cells. The 2-ml microfuge tubes containing the cells were shaken gently at room temperature for 1 h. After mixing thoroughly, the cells were harvested by centrifugation at 16000 *g* for 5 min and resuspended in 1 ml of acid-propanol (0.04 *M* HCl in isopropanol) by vortexing at highest speed for 30 s. After centrifugation at 400 *g* for 2 min, the supernatant was spectrophotometrically analyzed at 590 nm for formazan, a blue colored product formed when colorless MTT freely enters the cells and interacts with the electron transport chain located in the inner mitochondrial membrane.

Soluble protein determination

The Bio-Rad protein assay kit (Bio-Rad, Laboratories, Hercules, CA, USA) was used for protein determinations on the crude cell (200 mg fresh weight) extracts prepared in 500 μl Tris buffer Tris-HCl (50 m*M*, pH 8.4) containing 0.5 m*M* pyridoxal-5-phosphate, 0.1 m*M* EDTA and 5.0 m*M* dithiothreitol.

Ultrastructure (TEM) studies

Embryogenic suspension cultures of red spruce consisted of spherical clusters of meristematic cells with cylindrical suspensor cells extending from each cluster (see figure in Minocha et al. 1993). All ultrastructural analyses involved meristematic cells only. Three TEM studies were conducted: in all 3 studies, TEM of conventionally fixed cells (procedure below) was used to determine effects of Al on cell ultrastructure; in the second study, correlative stereology measurements were made in conjunction with the electron microscopy to determine significant structural changes in Al-treated cells; in the third study, EDX and TEM were performed on cells preserved by FS (see procedure in following section) to determine potential apoplastic or symplastic sites of Al accumulation.

In preparation for conventional (glutaraldehyde) preservation, the cells were collected after 24 h of Al exposure from each treatment flask onto Miracloth using vacuum filtration, and the unwashed pellet was placed in a 10-ml beaker to which 3 ml of 3% (w/v) Bacto agar (Difco Laboratories, Detroit, MI, study 1 and 2) or 1.5% agarose (w/v) (FMC BioProducts, Rockland, ME, Sea Plaque, low melting point, GTG, study 3) in 0.1 *M* phosphate buffer, pH 7.0 (freshly autoclaved and maintained at 40°C in a water bath), was added. Once the pellet solidified in the beaker, it was carefully removed to a clean Petri dish and cut into quarters. The pellet pieces were transferred into plastic vials labeled by treatment, and 9 ml of 3% (v/v) glutaraldehyde (EM Sciences, Fort Washington, PA) in 0.1 *M* phosphate buffer, pH 7.0, was added to each vial (enough to cover the material). The cell pellets were incubated for 3–4 h at room temperature in the dark, washed 4 times each with 10 ml of phosphate buffer and shipped overnight to the Delaware, OH Forest Service Laboratory for further processing. Thus these cells were in contact with Al for 24 h before they were preserved. The pellets were then subdivided into 2-mm^3 pieces, post-fixed in 2% (w/v) osmium tetroxide (OsO_4) for 2 h at 4°C, dehydrated in a graded ethanol series (30–100%) (v/v), and embedded in a PolyBed-Araldite epoxy resin mixture. Ultrathin sections (90 nm) of the resin-embedded cell pellets were cut with a diamond knife on LKB ultramicrotome, collected on copper (Cu) grids and stained with 4% (w/v) uranyl acetate and Reynold's lead citrate. The cells from each treatment were examined and photographed with a JEOL JEM-1010 transmission electron microscope operated at 80 kV. Eight to 10 replicate tissue blocks were sectioned per treatment and 20–50 thin sections per treatment were examined.

EDX study

In the third study, red spruce cells from each treatment were collected as described above and placed in 1.5% (w/v) agarose made in sterile 1/2 LM growth medium instead of phosphate buffer. The tissue embedded in agarose was shipped the same day in the appropriate spent media for each treatment for FS processing to the Center for Electron Optics, Michigan State University, East Lansing, MI, USA. These cells were thus in contact with Al for approximately 48 h (48 h Al treatment) before being fixed via FS. For FS preservation, small (< 0.5-mm^3) portions of agarose-solidified cell pellets were jet-frozen in liquid propane at -170°C. The frozen cell pellets were immersed immediately in the FS fixative [1% chromium trioxide (CrO_3) dissolved in acetone (w/v)], chilled with liquid nitrogen (-196°C); pellets were then transferred in vials to a container of isopropanol and dry ice and allowed over the next 3 days to return to room temperature. The Cr-fixed cell pellets were rinsed in anhydrous acetone over a 4 h period and embedded gradually in Spurr's epoxy resin (Spurr 1969). Sections (120–150 nm thick) of the cell pellets cut using the ultramicrotome were transferred singly to 200-mesh Cu grids. Six replicate tissue blocks per treatment were sectioned, and 30 tissue sections per treatment were analyzed for element content. EDX analysis of sections was performed in a JEOL JEM-1010 TEM equipped with a Link ISIS microanalysis system (Oxford Instruments Ltd., Buckinghamshire, UK) utilizing a Link Pentafet Si(Li) detector. TEM conditions for EDX were kept constant: 80 kV accelerating voltage; beam spot size 8; current density 2.0 pA cm^{-2}; goniometer tilt 30° towards the detector; magnification at $50000\times$. Each spectrum was collected for 100 s (live detector time). For each treatment, at least 20 spectra from each cellular component (e.g., cell wall, nucleus, vacuole) were collected from cells showing no visible disruptions in cell wall or plasma membrane integrity. Significant element peaks (i.e., area under peaks that were significantly greater than background) for each cellular component were identified by the Link Systems AUTO-Identification program (Link ISIS Operator's Manual Rev. 3.0, Copyright 1995, Oxford Instruments Ltd., Microanalysis Group, High Wycombe, Buckinghamshire, UK). Elements exhibiting characteristic X-ray energy (keV) emission lines were: Al (Kα, 1.487); phosphorus (P) (Kα, 2.014); iron (Fe) (Kα1, 6.404; Kβ1, 7.058); calcium (Ca) (Kα1, 3.692); sulfur (S) (Kα1, 2.308); chlorine (Cl) (Kα1, 2.622). Additional elements detected in all spectra include Cu (Kα, 8.048; Kβ, 8.905; Lα, 0.93) from the support grid, Cr (Kα1, 5.415; Kα2, 5.406; Kβ1, 5.947) from the fixative used, oxygen (O) (Kα1, 0.525), and carbon (C) (Kα1, 0.277).

Stereology studies

Ultrathin (90-nm) sections of red spruce cells (preserved by conventional fixation for TEM in study 2) were photographed at magnifications of 4000 and $10000\times$, print magnifications of 10800 and $27000\times$, respectively, and used for stereological measurements. At $10800\times$, 10 whole cells per treatment were photographed (total, 30 pictures). At $27000\times$, 3 photographs of different portions of 10 cells per treatment were photographed (total, 90 pictures).

The volume of an organelle per unit of cell volume (Vv, volume density) was calculated from micrographs at $10800\times$ magnification using the relationship:

$$Vv = 1/n \sum_{i=1}^{n} \left(\frac{Pt_{\alpha(i)}}{Pt_{\alpha(i)}} \right)$$

where Vv is the volume density of object, n is number of micrographs examined, Pt_{α} is the number of points from a point counting grid (Weibel, 1979) falling in the profile of interests (e.g., mitochondria) and Pt_{β} is the number of points falling within the containing volume (e.g., cell).

The surface area of membranes per unit of cell volume (Sv, surface density) was calculated from micrographs at 27000 × magnification using the following relationship:

$$Sv = \left(\frac{2}{k_1 \times d}\right) \frac{\sum_{i=1}^{n} Ia_{\alpha(i)}}{\sum_{i=1}^{n} Pt_{\alpha(i)}}$$

where Sv is the surface density of the membranes of interest, k is a constant based on the type of measuring grid used (Merz curvilinear = $\pi/2$; Weibel, 1979) and d is distance between points on Merz grid normalized to μm (Fagerberg, 1988), Ia_{α} is the number of intersections of the membrane with the curvilinear grid, and Pt_{β} is the number of grid points falling within the containing structure (e.g., cell).

Vv and Sv are terms used widely in the literature associated with stereology. They describe the percent of the mean cell volume occupied by an organelle or the surface area of a membrane per unit cell or organelle volume.

Standardized mean cell volume was calculated by photographing 2 μm-thick sections of tissue from study 2. The resulting 2 × 2 slides (n = 7 for control; n = 8 for 0.2 m*M* Al; n = 12 for 0.5 m*M* Al) were projected onto a point counting grid superimposed on a frosted glass screen at a pre-determined magnification. The nuclear profiles projected were measured with a micrometer and a mean area was calculated. The mean volume of the nucleus was then calculated based on the geometric model of a nucleus as a sphere. From this, standardized mean cell volumes were calculated by multiplying the mean nuclear volume times $1/Vv_{nucleus}$. This yielded an estimate of standardized mean cell volume. Standardized organelle volumes and membrane surface areas were then calculated by multiplying their Vv or Sv values times the calculated standardized mean cell volume for each treatment. The standardized mean cell volume could not be calculated directly because there is no good geometric model that could be applied for cell shape.

Statistical analyses

Linear regression analyses were performed to establish the strength and significance of relationships between two different variables using Excel 97™ (Microsoft Corporation, Roselle, IL). Data for each variable were analyzed as a series of one-way analysis of variance (ANOVA) to determine whether statistically significant differences occurred between control and Al-treated cells. When *F* values for one-way ANOVA were significant, differences in treatment means were tested by Tukey's multiple comparisons test. ANOVA and Tukey's tests were performed with Systat for Windows, version 7.01 (SYSTAT Inc., Evanston, IL, USA), and a probability level of 0.05 was used for most tests unless specified otherwise. Surface to volume and Vv ratios were tested for significant differences using INSTAT™ (Graphpad, San Diego, CA, USA) statistics program.

Results

Al effects on mitochondrial activity, cell viability, growth and soluble proteins

By 48 h, treatment of cells with Al resulted in a decrease in the following: (1) mitochondrial activity; (2) cell viability as measured by an increase in absorbance at 600 nm; (3) fresh weight indicating growth inhibition (Fig. 1). Cellular content of soluble proteins increased, particularly at 48 h, in Al-treated cells (Fig. 1). The change in soluble proteins was not always dose dependent at 48 h after Al addition. Unlike the data presented in Fig. 1, in some experiments, there was no further increase in soluble proteins by addition of 1.0 m*M* Al. A significant correlation was observed between cell growth, viability and mitochondrial activity in response to Al exposure.

Ultrastructure (TEM)

Spherical clusters of red spruce embryogenic cells that were not exposed to Al (control treatment) exhibited characteristics of actively growing meristem cells: thin primary cell walls; cytoplasm filled with cellular organelles; large circular nuclei and small vacuoles that occasionally contained small amounts of dense material (Fig. 2). Addition of Al to the medium resulted in increased cellular vacuolation accompanied by deformation of the nucleus, giving the impression of a possible reduction in nuclear size, especially at the 0.5 m*M* Al level (Fig. 3). The dense material in vacuoles increased in amount and density in cells grown at 0.2 (data not shown) and 0.5 m*M* Al (Fig. 3). Plastids in cells from all treatments had discrete, dense regions (data shown only for control and 0.5 m*M* Al, arrowheads; Figs 2 and 3).

Two distinct cellular disturbances were seen only in the outer concentric layer of cells from embryogenic cell clusters treated with 0.5 m*M* Al. First, plasma membrane separation from the cell wall was observed in approximately 10% of these outer layer embryogenic cells (Fig. 4); the cytoplasm, however, appeared normal. Secondly, in other cells in the outer concentric layer of clusters, the cytoplasm of approximately 5% of the cells was darkened and granular, and mitochondria and endoplasmic reticulum (ER) were swollen (Fig. 5). In addition, the part of the cell wall in contact with the medium appeared more dense, and cellular debris (probably from deteriorated cells) adhered to this cell wall.

Cells prepared by FS (Figs 6 and 7) displayed ultrastructural characteristics similar to those prepared by the conventional TEM method (seen in Figs 2–5). Freeze-substituted cells at 0.2 and 0.5 m*M* Al had increased amounts of electron-dense material in vacuoles (Fig. 6; 0.5 m*M* Al) compared to control cell vacuoles, and the granular, dense regions observed in plastids from Al-treated cells (Fig. 7; 0.5 m*M* Al) were similar to those seen in plastids from control cells.

EDX

A summary of significant elements detected by EDX in cellular components of freeze-substituted red spruce embryogenic cells grown in media containing 0, 0.2 or 0.5 m*M* Al for 48 h is given in Table 1. To be ranked at the 'high' detection level, an element must have been detected in significant quantity (as determined by the AUTO-Identification program used in this system) in greater than 30% of all spectra analyzed; 'low' detection level of an element resulted when a significant peak was detected in fewer than 30% of the spectra analyzed. Not listed in Table 1 are elements that had small but identifiable spectral peaks that were not categorized as significant by the AUTO-Identification program.

Al was detected in cell walls (i.e., the apoplast) of cells grown in medium containing 0.5 m*M* Al (Fig. 8A); Al was never detected in the absence of P in spectra collected from cell walls. At 0.2 m*M* Al, P was the only significant element detected in cell walls (Fig. 8B); however, an identifiable (but not significant) Al peak was observed in 50% of the spectra collected (e.g., Fig. 8B). By contrast, in control cells no significant elemental peaks were detected in cell walls (Table 1). Therefore, the concentration of Al in cell walls increased as the concentration in the medium increased.

Symplastic cell regions in which elements were detected in significant quantities included the cytoplasm, nucleus, vacuolar dense material and the discrete granular compounds in plastids (Table 1). At 0.2 m*M* Al treatment, Al was detected in significant amounts in 25% of the spectra collected from the cytoplasm and from the granular compounds located in plastids (Table 1, low detection). At 0.5 m*M* concentration, Al was detected in 50% of the spectra collected from cytoplasm and plastids (Table 1, high detection) and also in 20%

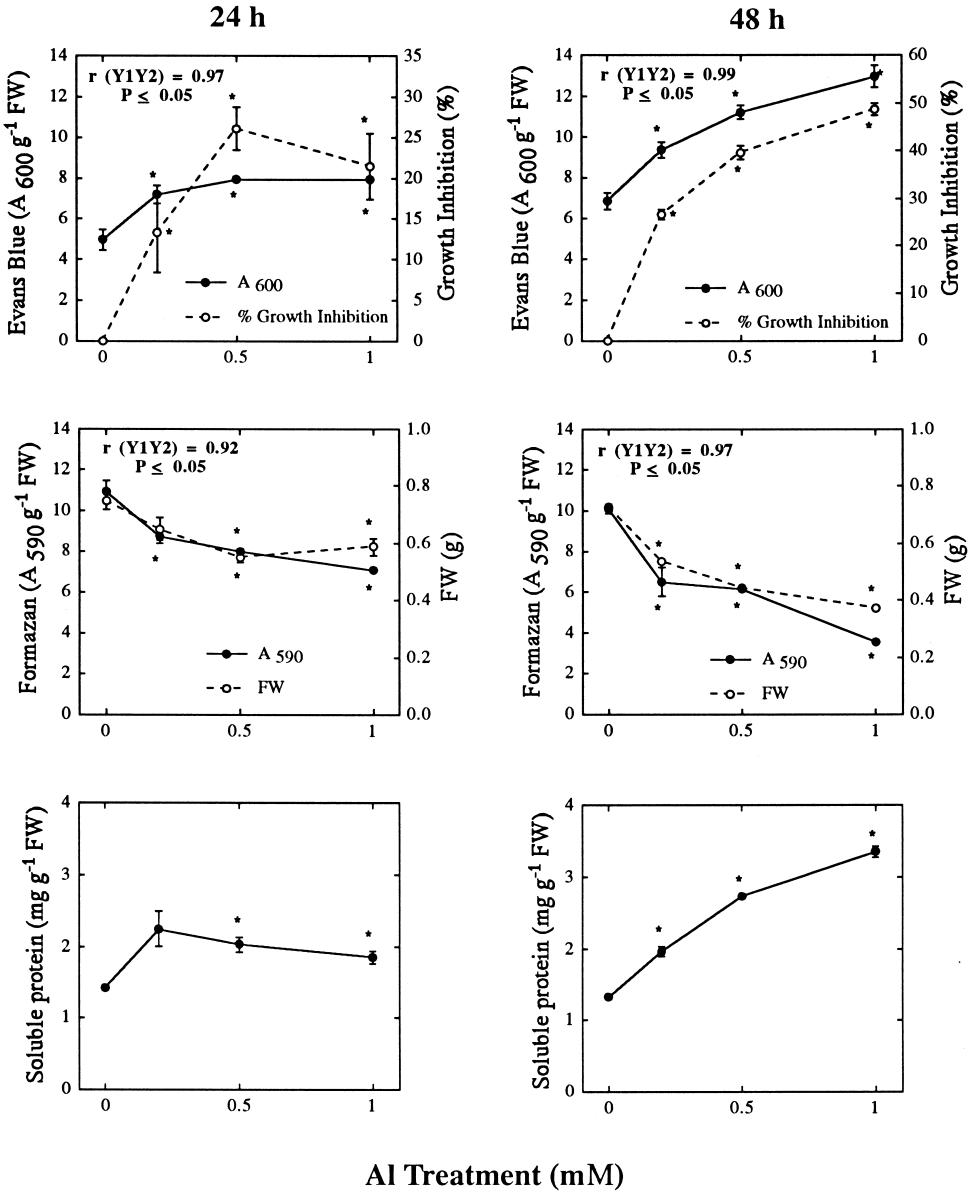

Fig. 1. Effects of addition of 0, 0.2, 0.5 and 1.0 m*M* $AlCl_3$ to 3-day-old suspension cultures of red spruce on fresh weight, plasma membrane integrity (Evans blue absorbance), mitochondrial activity (formazan absorbance) and soluble protein. The growth media for this set of experiments contained Fe-EDTA instead of sequestrene. Thus the effective concentrations of monomeric Al were the same as added and as shown on the figure. Values are mean ± SE of 4 replicates. Correlation values are between two dependent variables depicted on the graph. * Significant differences between control cells and Al-treated cells at $P \leq 0.05$. The data for 24 and 48 h come from two separate experiments.

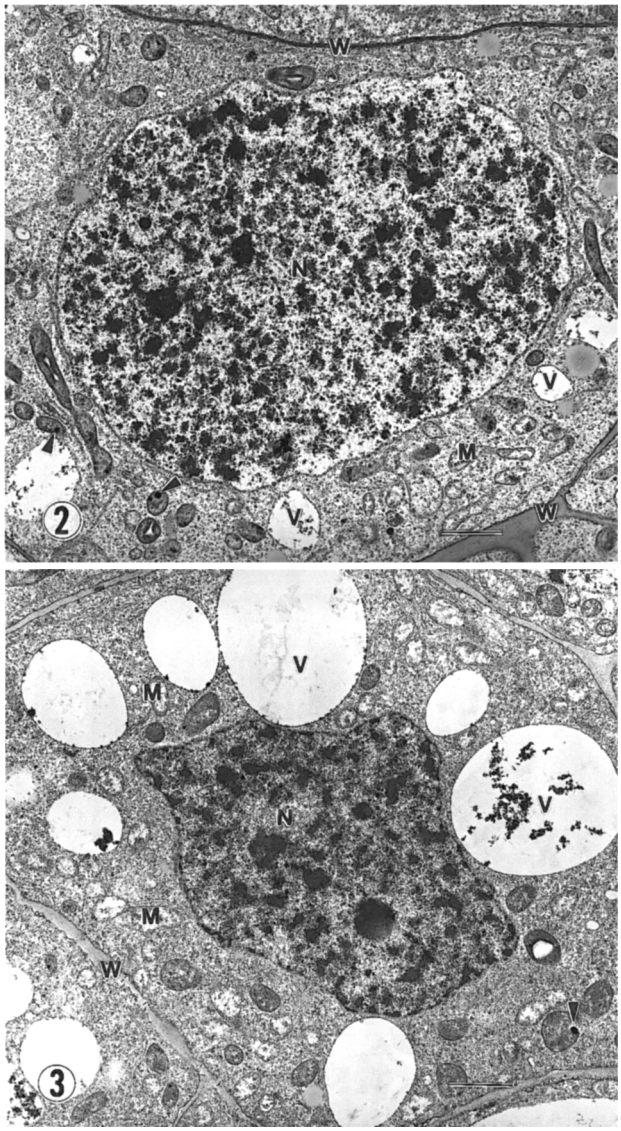

Figs 2 and 3. Effect of Al on red spruce embryogenic cell ultrastructure after 24 h exposure, following conventional (glutaraldehyde) fixation. **Fig. 2.** Control. Thin cell walls (W) surround cytoplasm filled with mitochondria (M), large central nucleus (N) and several small vacuoles (V). **Fig. 3.** 0.5 m*M* Al addition (effective monomeric Al concentration 0.23 m*M*). Vacuoles (V) increased in volume and often contained dense bodies. The nucleus (N) was irregularly shaped and appeared smaller in size relative to the total cell volume. Cell walls and cytoplasm appeared unaffected by Al treatment. Arrowheads, plastids containing dense bodies. Bars = 2 μm.

of the spectra from the contents of vacuolar material (Table 1, low detection). A comparison of representative spectra analyzing the dense granular material in a plastid from a cell exposed to 0.5 m*M* Al (Fig. 8C) and from a control cell (Fig. 8D) revealed significant peaks of P, Al and Fe in the granular material from the Al-treated cell, but significant, peaks of P, Ca and Fe in material from the control cell. In this study, P was detected in significant amounts in all cell nuclei (Table 1). Although Al was not detected in significant quantity in the nuclei of any spruce cells analyzed, small peaks of Al (but below significance level) were observed in spectra from nuclei of 0.5 m*M* Al-treated cells ($< 30\%$ frequency; data not shown).

Stereology

The treatment of red spruce cells with Al altered the cell structure. In the Al-treated cells, there was a reduction in the Vv (organelle volume as a percentage of the total cell volume in $\mu m^3\ \mu m^{-3}$) of the nuclear compartment and an increase in the Vv of the vacuolar compartment (Table 2). The Vv of the nucleolar and mitochondrial compartments did not vary significantly between the Al-treated and control cells (Table 2).

Membrane systems within the cell also changed following Al treatment. The Sv (organelle surface area per unit of total cell volume in $\mu m^2\ \mu m^{-3}$) of the ER was significantly lower in cells exposed to 0.5 m*M* Al compared to controls (Table 3). The Sv of the Golgi cisternae was also significantly lower in 0.2 and 0.5 m*M* Al-treated cells as compared to control cells (Table 3).

Standardized volumes and surface areas of organelles were calculated to assess actual size changes that took place during exposure to Al. Although the Vv data presented above showed a decrease in the Vv of the nuclear compartment relative to whole cell volume (Table 2), based on standardized mean cell volume, there was no significant change in nuclear volume in cells treated with Al (Table 2). In contrast, the actual volume of the nucleolus was greater in the Al-exposed cells (Table 2). Mitochondria also showed higher standardized mean volumes (SMV) in cells exposed to Al, the highest increase being observed with 0.2 m*M* Al (Table 2). The vacuolar compartment followed the trend set in the Vv data and showed a large dose-dependent increase in volume with Al treatment (Table 2). Vacuolar volume per mean standardized cell increased 463% in the 0.2 m*M* and 758% in the 0.5 m*M* Al-treated samples relative to the controls.

Although the Sv ($\mu m^2\ \mu m^{-3}$) of the ER was lower in 0.5 m*M* Al-exposed cells, the actual surface area per standardized mean cell volume increased with increasing Al concentration. Similar observations were made with the Golgi membrane surface area (Table 3). The ER surface area per mean cell increased 76 and 34% in the 0.2 and 0.5 m*M* Al-treated cells, respectively, while the Golgi surface area increased by 14 and 30% in the same respective samples.

Discussion

In the present study, similar to the work published earlier with tobacco cells (Ikegawa et al. 1998), cell viability was directly correlated with loss of fresh weight caused by Al treatment. Thus the biochemical data showed that about 30% of the cells treated with 0.5 m*M* Al for 48 h may have lost membrane integrity before the total disruption of the dying cells. The apparent loss of fresh weight despite the increase in cellular volume in the stereological study may in part be explained by death and decay of the above mentioned fraction of cells due to Al exposure. Loss of cell

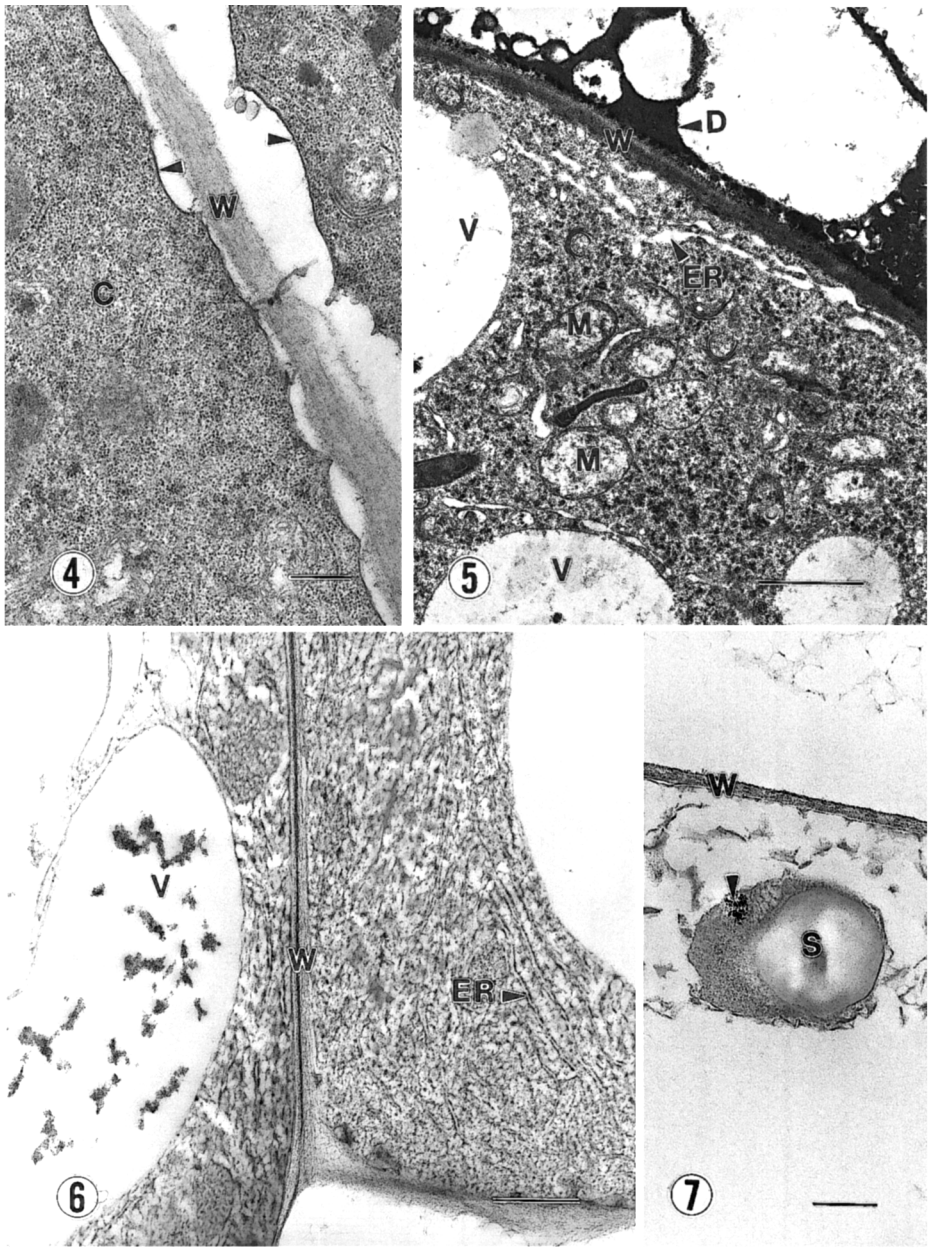

Figs 4 and 5. Cellular disturbances seen only in 5–10% of the cells located in the outer concentric layer of meristematic cell clusters treated with 0.5 m*M* Al (effective monomeric Al concentration 0.23 m*M*) for 24 h, conventional fixation. **Fig. 4.** The plasma membrane (arrowheads) has separated from the cell wall (W). Cell cytoplasm appears unaffected. Bar = 500 nm. **Fig. 5.** Cell debris (D) adhered to dense outer wall (W) of embryogenic cell. Cell contained swollen endoplasmic reticulum (ER) and mitochondria (M) with few internal membranes (cristae). Bar = 2 μm.

Figs 6 and 7. Red spruce cells treated with 0.5 m*M* Al (effective monomeric Al concentration 0.23 m*M*) for 48 h before fixation by FS. **Fig. 6.** Portions of two cells separated by cell wall (W). Cell vacuole (V) contained electron-dense bodies. Cell organelles, such as endoplasmic reticulum (ER), in the cytoplasm appeared unaffected by Al treatment. Bar = 1 μm. **Fig. 7.** Plastid, containing large starch grain (S) and electron-dense material (arrowhead) that appeared granular. W, cell wall. Bar = 500 nm.

viability, decreased growth and the disruption of cellular microtubules have been reported in roots of wheat (Sasaki et al. 1997) and soybean (Kataoka et al. 1997) exposed to Al. Lazof et al. (1994, 1996) concluded that early metabolic responses to external Al, such as inhibition of cell division, cell extension or nutrient transport, occur not only at the root tip, but also within mature roots and involve direct suppression of cell function by intracellular Al. Ishikawa and Wagatsuma (1998) reported that in Al-sensitive species (pea and barley), temporary contact with Al ions irreversibly altered the plasma membrane of root tip cells. This binding in turn made the membrane leaky and rigid. It can thus be argued that the membrane permeability changes result from Al-induced extracellular lesions with Al then entering the symplast. The present data do not discount this possibility.

There was no apparent relationship between mitochondrial size and activity. Even though actual mitochondrial volume increased (though not in a dose-dependent manner) in response to Al treatment, the mitochondrial activity in these cells decreased significantly in a dose-dependent manner. The presence of fewer cristae in the mitochondria (Fig. 5) may be related to decreased mitochondrial activity in the Al-treated cells. In contrast to a previous report with tobacco cells (Ikegawa et al. 1998), decreased mitochondrial activity was significantly correlated to a loss of fresh weight within the 48 h period. In the Ikegawa et al. (1998) report, a correlation between percent growth inhibition and mitochondrial activity was studied after treating the cells with Al for 18 h and subsequently allowing the cells to recover and grow for 7 days after Al removal and prior to conducting

Table 1. Summary of elements showing significant emission lines in cellular components of red spruce embryogenic cells that were in contact with growth media containing 0, 0.2 or 0.5 m*M* Al (effective monomeric Al concentrations 0, 0.09 and 0.23 m*M*, respectively) for 48 h and then preserved by FS. Link Systems AUTO-Identification program was used to determine the significance of a peak. Two levels of detection are listed for each element: (1) low level, significant peak detected in fewer than 30% of the spectra collected; (2) high level, significant peak detected in more than 30% of the spectra collected. For each treatment, 20 spectra of each cell component from different spruce cells were collected.

Cellular component	Control		0.2 m*M* Al		0.5 m*M* Al	
	Low	High	Low	High	Low	High
Cell wall	–	–	P	–	–	P, Al
Cytoplasm	P, Fe, S	–	S, Al, Cl	P	S, Cl	P, Al
Plastid (granular compound)	Cl, S	P, Fe, Ca	Cl, Al	P, Fe	S, Cl, K	P, Fe, Al
Vacuole (dense material)	P	–	–	P	Fe, S, Al	P
Nucleus	–	P	S, Cl	P	S, Cl	P

the assays. In the present study, however, assays were conducted and cell weights taken immediately after 24 or 48 h of Al exposure.

Soluble protein levels increased substantially in red spruce cultures in response to Al treatment. Plants are known to respond to various forms of abiotic and biotic environmental stress by changes in the levels of proteins, such as heat-shock proteins, dehydrins, osmotin, antioxygenic enzymes, cold regulated (COR) proteins, dessication stress protein (DSP), late embryogenesis abundant (LEA) proteins and polyamine biosynthetic enzymes (Close and Bray, 1993, Tzvi et al. 1999). Weidner and Kraus (1987) reported increases in soluble protein levels in the needles of 'declining' red spruce (*Picea abies)* trees, but found no increases in the amount or activity of the most abundant leaf protein, Rubisco. This observation indicates that this increase in the protein pool was probably not connected with plant growth, i.e., photosynthesis. The increase in the total soluble protein pool observed in the present study may be indicative of changes in the level of induction and/or expression of some stress related genes. In addition, some of this increase may also be due to degrading organelles inside 'non-leaky' plasma membranes. However, the proteins from leaky plasma membranes were lost when these cells were washed twice on miracloth before collection.

The EDX data presented in this paper are supported by the previous findings of Zhou et al. (1995) and Minocha et al. (1996), which showed an increase in the cellular concentration of Al in Al-treated cells. These earlier studies, however, did not test if Al was bound to the cell walls or actually entered the symplast. The present data suggest movement of Al into the symplast. In 0.5 m*M* Al-treated cells, Al was detected by EDX in dense regions of the cell walls, cytoplasm and plastids. In the vacuoles, significant peaks of Al were detected, but in less than 30% of the spectra examined. The reason for overall low frequency of Al detection in the organelles from inner cell layers even in the presence of 0.5 m*M* Al may be due to the type and complexity of the embryogenic cell clusters, which may have slowed the rate of Al movement to the inner cell layers. Whallon et al. (1989) have reported that a realistic minimum concentration detectable by EDX may be approximately 0.1% by weight. It is probable that Al ions entering the cells were sufficiently concentrated (or complexed with organic or inorganic compounds) to be detectable in the dense areas. Taylor et al. (2000) reported that after 12 to 24 h of Al exposure, cell walls, cytoplasm and vacuoles of *Chara corallina* were Al-saturated (indicating movement of Al across plasma membrane). A similar Al-saturation/concentration may have occurred in electron-dense regions of these red spruce cells after 48 h. In translucent (non-dense) regions of the cells analyzed by EDX, Al may have been too diffuse for significant detection, especially in 0.2 m*M* Al-treated cells. The distinct (but not significant) peaks of Al observed in many of the spectra collected from cells of this treatment suggest that the lack of a significant Al peak does not completely exclude the possibility of Al presence. Although absolute concentration of Al was not determined by the semiquantitative EDX detection method used, analysis of cellular thin sections indicates that Al movement into the symplast probably had occurred.

In the present study, Al was not found in each spectrum collected from cell walls, although many studies report this is the primary location of Al accumulation. Several factors may account for the lack of consistent Al detection in cell walls. First, the EDX spectra were collected from individual regions on randomly selected cell walls. It is possible that Al may not have been evenly distributed in the cell walls, i.e., possible 'patchy' distribution with the greatest quantity of Al associated with P in the dense portions of cell walls. Secondly, spectra were collected randomly from cell walls in all layers of the embryogenic clusters. Cell walls from the outer concentric layer in direct contact with the Al-containing medium generally had a higher frequency of Al detection than cell walls from inner cell layers not in direct contact with the medium. It is interesting to note that Vázquez et al. (1999) detected Al in cell walls of Al-tolerant maize after 4 h, but not after 24 h (a lowering of insoluble apoplastic Al), indicating that Al may not always remain in large quantities in the apoplast. The authors suggested that this may be a mechanism by which these cells develop resistance to Al. The absence of a significant quantity of Al in cell walls of 0.2 m*M* Al-treated cells may also suggest that this red spruce cell line is relatively tolerant to this concentration of Al as compared to other species where studies have shown that most of the Al is bound to cell walls. However, a treatment with the higher concentration of Al (0.5 m*M*) resulted in significant quantities of Al in the cell wall.

Previous reports have shown that Al phosphate precipitates in the cell walls or other cellular components, including

vacuoles in the symplast (Macklon and Sim 1992, Marienfeld and Stelzer 1993, Marienfeld et al. 1995, Kataoka et al. 1997, Vázquez et al. 1999). Campbell (1999) reported that, in alfalfa roots, Al-tolerant clones had less free Al in the epidermis and internal root tissue than Al-sensitive clones because some of this Al in Al-resistant clones may have been bound to low molecular weight proteins and organic acids. Cell cultures of spruce also were shown to have dose-dependent increases in the cellular levels of Al and P (apoplastic plus symplastic) when exposed to Al (Minocha et al. 1996). In the present study, P was always detected at a higher frequency in cellular components of Al-treated cells compared to control cells. Al and P were consistently detected in the same cellular regions in EDX spectra. However, further data are needed to provide conclusive evidence that Al is sequestered by the cells as an Al phosphate complex. Al is generally known to compete with cations, such as Ca, for binding sites in cell walls and cytoplasmic regions (Horst 1995). The detection of Al in association with Fe and P in plastids of Al-treated cells instead of Ca with Fe and P, as found in control cells (Fig. 8C,D; Table 1), may be an example of this ion competition.

Al altered the basic architecture of the cell as indicated by changes in the Vv and Sv of cellular components in Al-treated cells compared to control cells. Based upon standardized mean cell volume data, it can be concluded that Al treatment increased the volume of red spruce cells. This increase was likely facilitated by increases in the vacuolar compartment size, perhaps as a result of turgor changes within the cell. Increased vacuolation may have been important in 'compartmentalizing Al' thus lessening its negative effects when it entered the cytoplasm. Vázquez et al. (1999) have shown the accumulation of Al in the vacuoles of root cells in an Al-tolerant maize variety and Taylor et al. (2000) demonstrated saturating levels of Al in the vacuoles of *Chara* cells within 12–24 h. In both of these studies, however, the authors did not measure the size of the vacuoles. Contrary to the above mentioned Al effects on cell volume and vacuolar swelling, at 0.5 m*M* Al, a relatively small number of cells in the outer concentric layer of embryogenic cell clusters showed separation of the plasma membrane from the cell wall (Fig. 4); this effect may have been due to changes in membrane permeability properties because the cells were in direct contact with this high concentration of

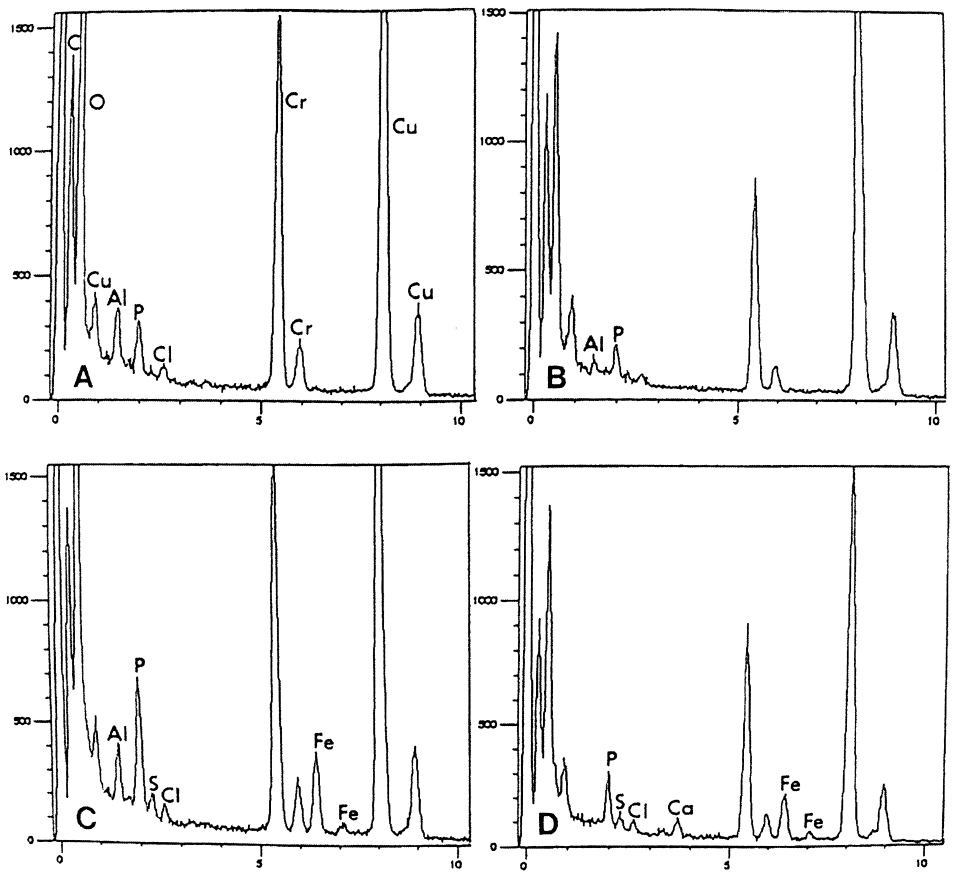

Fig. 8. A–D. Representative EDX spectra collected from subcellular components of red spruce embryogenic cells that were in contact with growth media containing appropriate concentrations of Al for 48 h and then freeze-substituted. Markers on horizontal axis are X-ray energy levels (0–10 keV). Markers on vertical axis are total counts (0–1500) 100 s^{-1}. Peaks constant in all spectra (labeled only in A) are Cu (from the support grid), Cr (the fixative used), O and C. **A**. Cell wall, 0.5 m*M* Al (effective monomeric Al concentration 0.23 m*M*). Significant Al and P peaks were seen, and a small Cl peak (not significant, as determined by the Link Systems AUTO-Identification program) also was present. **B**. Cell wall, 0.2 m*M* Al (effective monomeric Al concentration 0.09 m*M*). A significant P peak was detected in most cell walls. An identifiable, but not significant, Al peak also was present. **C**. Spectrum of dense granular material from plastid in Fig. 7 (0.5 m*M* Al). Al, P and Fe were present in significant amounts; identifiable, but insignificant, peaks of S and Cl were also detected. **D**. Spectrum of dense material from plastid in a cell grown without Al (control). Significant peaks of P, Fe and Ca were present. Similar to spectrum in C, small peaks of S and Cl were detected.

Table 2. Vv (the ratio of the organelle volume compared to the cell volume) of various organelles and SMV of cell and organelles in control and Al-treated cells. The cells were cultured in growth media containing 0, 0.2 and 0.5 m*M* Al (effective monomeric Al concentrations 0, 0.09 and 0.23 m*M*, respectively) for 24 h and then preserved by conventional glutaraldehyde fixation. The data presented for Vv are mean ± SE. *Significant differences from the control mean for $P \leq 0.05$. Since SMVs were calculated using a model, Standard errors and significance levels for differences between treatments could not be determined. For more details on these calculations see Materials and methods. Note: Vv of nucleolus is a ratio of nucleolus volume to nucleus volume.

Treatment	Whole cell	Nuclei	Nucleoli	Mitochondria	Vacuoles	Oil
Vv						
Control (n = 10)		0.31 ± 0.09	0.034 ± 0.018	0.074 ± 0.014	0.054 ± 0.016	0.008 ± 0.009
0.2 m*M* Al (n = 11)		0.182 ± 0.047*	0.087 ± 0.035	0.090 ± 0.013	0.179 ± 0.039*	0.002 ± 0.000
0.5 m*M* Al (n = 11)		0.177 ± 0.031*	0.080 ± 0.013	0.054 ± 0.017	0.262 ± 0.72*	0.003 ± 0.005
SMV (μm^3)						
Control (n = 7)	8 710	2 700	91	646	470	
0.2 m*M* Al (n = 8)	14 810	2 700	235	1 330	2 645	
0.5 m*M* Al (n = 10)	15 900	2 816	224	859	4 160	

Al. In addition, the debris adhering to walls of cells in the outer concentric layer (Fig. 5) may have been the disintegrated cell fragments that adhered to cell clusters during the pelleting procedure. The live cells that were still physiologically responding to Al exposure, on the other hand, showed an increase in both cell and vacuolar volume without any visible damage to the plasma membrane. Increased vacuolation in meristematic cells after Al exposure has been described in previous studies (McQuattie and Schier 1992, Schier and McQuattie 1995). Ikegawa et al. (2000) also found slight plasmolysis in Al-treated tobacco cells, suggesting that Al causes some minor morphological and functional changes in the plasma membrane. Furthermore, they reported that these plasma membranes remained intact (by measuring leakage of K ions).

The decrease in nuclear volume (Vv) in Al-treated cells was apparently due to an increase in whole cell volume in Al-treated cells. The irregular nuclear shape may be related to Al treatment or may be the result of increased vacuolation in the cytoplasm causing nuclear deformation. The relative proportion of total cell volume occupied by the nucleus decreased by 41 and 43%, respectively, in 0.2 and 0.5 m*M* Al-treated cells compared to the control cells (Table 2). The nucleoli, however, increased 156 and 135%, respectively, in the relative proportion they occupied of the nucleus volume in the Al-treated cells. In the case of the two membrane systems measured (ER and Golgi), the Sv values remained the same or decreased relative to control cells while in terms of actual surface area per standardized mean cell volume both systems increased (Table 3). These data indicate that the membrane systems did not grow proportionally (i.e., as fast as the cell volume increased), but both increased in the Al-treated cells as compared to the control cells. Both membrane systems are essential in building and targeting membranes (plasma membrane and tonoplast) for the cell. These membrane systems are linked together in the secretory pathway. Increases in Golgi and ER membrane surface due to Al exposure also may indicate possible increases in secretory activity to the plasma membrane or vacuolar compartments. ER membrane surface area increased by 76 and 34%, respectively, with 0.2 and 0.5 m*M* Al treatment while Golgi membrane surface areas only increased by 14 and 30% in the two concentrations. This difference in change in the surface area of Golgi and ER may indicate a change in the rate of Golgi turnover relative to ER.

Conclusion

Decreased growth/viability of red spruce cells following 24–48 h of Al exposure may be related to the decreased plasma membrane integrity and mitochondrial activity and to the visible loss of mitochondrial membranes. Although significant alterations in the surface area of cellular membranes (Golgi, ER, vacuoles) were detected, spruce embryogenic cells (with the exception of the outer concentric layer of cells) after exposure to Al remained visually intact when viewed by TEM. The detection of Al in intracellular compartments (cytoplasm, vacuoles, plastids) by EDX in the cells that appeared intact support the theory that Al is transported to the cell symplast without significant disruption of the cells. EDX analysis of Al-treated cells was used primarily to determine whether Al accumulated in intact cells after a relatively long exposure time (48 h). Whether Al caused microscopic lesions in the plasma membrane, allowing for Al to enter cells, was beyond the scope of this study and, for this red spruce embryogenic cell system, is yet to be determined. This research does show, however, that red spruce cells are relatively tolerant of high Al concentrations

Table 3. Sv (surface area of membranes per unit of cell volume) and standardized mean surface area (SMSA) of the ER and Golgi membranes. The cells were cultured in growth media containing 0, 0.2 and 0.5 m*M* Al (effective monomeric Al concentrations 0, 0.09 and 0.23 m*M*, respectively) for 24 h and then preserved by conventional glutaraldehyde fixation. The data presented for Sv are mean ± SE. *Significant differences from the control mean for $P \leq 0.05$. Since SMSAs were calculated using a model, Standard errors and significance levels for differences between treatments could not be determined. For more details on these calculations see Materials and methods.

Treatment	ER	Golgi
Sv		
Control (n = 36)	0.478 ± 0.02	0.188 ± 0.015
0.2 m*M* Al (n = 41)	0.494 ± 0.018	0.127 ± 0.011*
0.5 m*M* Al (n = 50)	0.352 ± 0.013*	0.134 ± 0.009*
SMSA (μm^2)		
Control (n = 7)	4 160	1 640
0.2 m*M* Al (n = 8)	7 310	1 880
0.5 m*M* Al (n = 10)	5 590	2 130

for 24–48 h, with the most severe symplastic disruptions only in the outer layer of embryogenic cells (i.e., those in direct contact with Al in the media).

Acknowledgements – The authors are thankful to Ms. Jacqueline Wood, Center for Electron Optics, Michigan State University, East Lansing, MI, USA for the FS processing of red spruce embryogenic cells. The authors will also like to thank Brian Pellerin for his help with the stereological work for standardized volume calculations. The use of trade, firm or corporation names in this publication is for the information and convenience of the reader. Such use does not constitute an official endorsement or approval by the US Department of Agriculture or the Forest Service of any product or service to the exclusion of others that may be suitable.

References

Campbell TA (1999) Magnetic resonance imaging of absorbed aluminum in alfalfa roots. J Plant Nutr 22: 827–834

Close TJ, Bray EA (1993) Plant responses to cellular dehydration during environmental stress. Curr Top Plant Physiol: Am Soc Plant Physiol Ser 10: 295

Cuenca G, Herrera R, Mérida T (1991) Distribution of aluminum in accumulator plants by x-ray microanalysis in *Richeria grandis* Vahl leaves from a cloud forest in Venezuela. Plant Cell Environ 14: 437–441

Driscoll CT (1984) A procedure for the fractionation of aqueous aluminum in dilute acidic waters. Intl J Environ Anal Chem 16: 267–283

Fagerberg WR (1988) Stereological techniques (Vv, Sv). In: Dawes CJ (ed) Biological Techniques for Scanning and Transmission Electron Microscopy: Theory and Practice. Ladd Publishers, Burlington, VT, pp 265–281

Horst WJ (1995) The role of the apoplast in aluminum toxicity and resistance of higher plants: A review. Z Pflanzenernaehr Bodenkd 158: 419–428

Huang JW, Shaff JE, Grunes DL, Kochian LV (1992) Aluminum effects on calcium fluxes at the root apex of aluminum-tolerant and aluminum-sensitive wheat cultivars. Plant Physiol 98: 230–237

Ikegawa H, Yamamoto Y, Matsumoto H (1998) Cell death caused by a combination of aluminum and iron in cultured tobacco cells. Physiol Plant 104: 474–478

Ikegawa H, Yamamoto Y, Matsumoto H (2000) Responses to aluminum of suspension-cultured tobacco cells in a simple calcium solution. Soil Sci Plant Nutr 46: 503–514

Ishikawa S, Wagatsuma T (1998) Plasma membrane permeability of root-tip cells following temporary exposure to Al ions is a rapid measure of Al tolerance among plant species. Plant Cell Physiol 39: 516–525

Kataoka T, Iikura H, Tomoko M (1997) Aluminum distribution and viability of plant root and cultured cells. Soil Sci Plant Nutr 43: 1003–1007

Kinraide TB (1998) Three mechanisms for the calcium alleviation of mineral toxicities. Plant Physiol 118: 513–520

Kochian LV (1995) Cellular mechanisms of aluminum toxicity and resistance in plants. Annu Rev Plant Physiol Plant Mol Biol 46: 237–260

Lazof DB, Holland MJ (1999) Evaluation of the aluminium-induced root growth inhibition in isolation from low pH effects in *Glycine max*, *Pisum sativum* and *Phaseolus vulgaris*. Aust J Plant Physiol 26: 147–157

Lazof DB, Goldsmith JG, Rufty TW, Linton RW (1994) Rapid uptake of aluminum into cells of intact soybean root tips. Plant Physiol 106: 1107–1114

Lazof DB, Goldsmith JG, Rufty TW, Linton RW (1996) The early entry of Al into cells of intact soybean roots. A comparison of three developmental root regions using seconday ion mass spectrometry imaging. Plant Physiol 112: 1289–1300

Lazof DB, Goldsmith JG, Linton RW (1997) The in situ analysis of intracellular aluminum in plants. Prog Bot 58: 112–159

Litvay JD, Johnson MA, Verma D, Einspahr D, Wayrauch K (1981) Conifer suspension culture medium development using analytical data from developing seeds. Inst Pap Chem Tech Pap Serv 115: 1–17

Ma FJ, Hiradate S (2000) Form of aluminum for uptake and translocation in buckwheat (*Fagopyrum esculentum*) Moench. Planta 211: 355–360

Macklon AES, Sim A (1992) Modifying effects of a non-toxic level of aluminum on phosphate fluxes and compartmentation in root cortex cells of intact ryegrass seedlings. J Exp Bot 43: 1483–1490

Marienfeld S, Lehmann H, Stelzer R (1995) Ultrasound investigations and EDX-analyses of Al-treated oat (*Avena sativa*) roots. Plant Soil 171: 167–173

Marienfeld S, Schmohl N, Klein M, Schröder WH, Kuhn AJ, Horst WJ (2000) Localisation of aluminum in root tips of *Zea mays* and *Vicia faba*. J Plant Physiol 156: 666–671

Marienfeld S, Stelzer R (1993) X-ray microanalyses in roots of Al-treated *Avena sativa* plants. J Plant Physiol 141: 569–573

Matsumoto H, Hirasawa E, Torikai H, Takahashi E (1976) Localization of absorbed aluminum in pea root and its binding to nucleic acids. Plant Cell Physiol 17: 127–137

McQuattie CJ, Schier GA (1990) Response of red spruce seedlings to aluminum toxicity in nutrient solution: Alterations in root anatomy. Can J For Res 20: 1001–1011

McQuattie CJ, Schier GA (1992) Effect of ozone and aluminum on pitch pine (*Pinus rigida*) seedlings: Alterations in the anatomy of mycorrhizae. Can J For Res 22: 1901–1916

Minocha R, Kvaalen H, Minocha S C, Long S (1993) Polyamines in embryogenic cultures of Norway spruce (*Picea abies*) and red spruce (*Picea rubens*). Tree Physiol 13: 365–377

Minocha R, Minocha SC, Long S, Shortle WC (1992) Effects of aluminum on DNA synthesis, cellular polyamines, polyamine biosynthetic enzymes, and inorganic ions in cell suspension cultures of a woody plant, *Catharanthus roseus*. Physiol Plant 85: 417–424

Minocha R, Shortle WC, Coughlin DJ, Minocha SC (1996) Effects of Al on growth, polyamine metabolism, and inorganic ions in suspension cultures of red spruce (*Picea rubens*). Can J For Res 26: 550–559

Minocha R, Shortle WC, Lawrence GB, David MB, Minocha SC (1997) A relationship among foliar chemistry, foliar polyamines, and soil chemistry in red spruce trees growing across the northeastern United States. Plant Soil 191: 109–122

Mosmann T (1983) Rapid colorimetric assay for cellular growth and survival: Application to proliferation and cytotoxicity assays. J Immunol Methods 65: 55–63

Olivetti GP, Etherton B (1991) Aluminum interactions with corn root plasma membrane. Plant Physiol 96 (Suppl): 142

Rengel Z (1992) Role of Ca in Al toxicity. New Phytol 121: 499–513

Rengel Z (1996) Uptake of aluminum by plant cells. New Phytol 134: 389–406

Rengel Z, Reid R (1997) Uptake of Al across the plasma membrane of plant cells. Plant Soil 192: 31–35

Sasaki M, Yamamoto Y, Matsumoto H, Feng MJ, Matsumoto H (1997) Early events induced by aluminum stress in elongating cells of wheat root. Soil Sci Plant Nutr 43: 1009–1014

Schier GA, McQuattie CJ, Jensen KF (1990) Effect of ozone and aluminum on pitch pine (*Pinus rigida*) seedlings: Growth and nutrient relations. Can J For Res 20: 1714–1719

Schier GA, McQuattie CJ (1995) Effect of aluminum on growth, anatomy, and nutrient content of ectomycorrhizal and nonmycorrhizal eastern white pine seedlings. Can J For Res 25: 1252–1262

Spurr AR (1969) A low-viscosity epoxy resin embedding medium for electron microscopy. J Ultrastruct Res 26: 31–43

Steer MW (1981) Understanding Cell Structure. Cambridge University Press, New York, NY, pp 1–126

Taylor GJ, Mcdonald-Stephens L, Hunter DB, Bertsch PM, Elmore D, Rengel Z, Reid RJ (2000) Direct measurement of aluminum uptake and distribution in single cells of *Chara corallina*. Plant Physiol 123: 987–996

Tzvi T, Wangxia W, Arie A (1999) Genetic transformation of populus toward improving plant performance and drought tolerance. In: Jain SM, Minocha SC (eds) Molecular Biology of Woody Plants, Vol. 2. Kluwer Academic Publishers, Dordrecht, pp 135–160

Vázquez MD, Poschenreider C, Corrales I, Barceló J (1999) Change in apoplastic aluminum during the initial growth response to aluminum by roots of a tolerant maize variety. Plant Physiol 119: 435–444

Weibel ER (1979) Stereological methods. In: Wiebel ER (ed) Practical Methods for Biological Morphometry, Vol. 1. Academic Press, New York, NY, pp 1–415

Weidner M, Kraus M (1987) Ribulose-1,5-bisphosphate carboxylase activity and influence of air pollution in spruce. Physiol Plant 70: 664–672

Whallon JW, Flegler SL, Klomparens KL (1989) Energy-dispersive x-ray microanalysis. BioScience 39: 256–259

Yamamoto Y, Hachiya A, Matusumoto H (1997) Oxidative damage to membranes by a combination of aluminum and iron in suspension-cultured tobacco cells. Plant Cell Physiol 38: 1333–1339

Zhang G, Taylor G (1989) Kinetics of aluminum uptake by excised roots of aluminum-tolerant and aluminum-sensitive cultivars of *Triticum aestivum* L. Plant Physiol 91: 1094–1099

Zhang G, Slaski JJ, Archambault DJ, Taylor GJ (1997) Alterations in plasma membrane lipids in aluminum-resistant and aluminum-sensitive wheat genotypes in response to aluminum stress. Physiol Plant 99: 302–308

Zhou X, Minocha R, Minocha SC (1995) Physiological responses of suspension cultures of *Catharanthus roseus* to aluminum: Changes in polyamines and inorganic ions. J Plant Physiol 145: 277–284

Edited by J. K. Schjørring